applied sciences

MDPI

Article

Interleukin 6 Plays a Role in the Migration of Magnetically Levitated Mesenchymal Stem Cells Spheroids

Jake Casson, Sam O'Kane, Carol-Anne Smith, Matthew John Dalby and Catherine Cecilia Berry *

Centre for Cell Engineering, Institute of Molecular, Cell and Systems Biology (IMCSB), The University of Glasgow, Joseph Black Building, University Avenue, Glasgow G12 8QQ, UK; j.casson.1@research.gla.ac.uk (J.C.); samokane1992@gmail.com (S.O.); carol-anne.smith@glasgow.ac.uk (C.-A.S.); matthew.dalby@glasgow.ac.uk (M.J.D.)

* Correspondence: Catherine.Berry@glasgow.ac.uk; Tel.: + 44-141-330-8400

Received: 9 January 2018; Accepted: 6 March 2018; Published: 11 March 2018

Abstract: Mesenchymal stem cells (MSCs) reside quiescently within a specialised 'niche' environment in the bone marrow. However, following appropriate signalling cues, MSCs mobilise and migrate out from the niche, typically toward either sites of injury (a regenerative response) or toward primary tumours (an intrinsic homing response, which promotes MSCs as cellular vectors for therapeutic delivery). To date, very little is known about MSC mobilisation. By adopting a 3D MSC niche model, whereby MSC spheroids are cultured within a type I collagen gel, recent studies have highlighted interleukin-6 (IL-6) as a key cytokine involved in MSC migration. Herein, the ability of IL-6 to induce MSC migration was further investigated, and the key matrix metalloproteinases used to effect cell mobilisation were identified. Briefly, the impact of IL-6 on the MSC migration in a two-dimensional model systems was characterised—both visually using an Ibidi chemotaxis plate array (assessing for directional migration) and then via a standard 2D monolayer experiment, where cultured cells were challenged with IL-6 and extracted media tested using an Abcam Human MMP membrane antibody array. The 2D assay displayed a strong migratory response toward IL-6 and analysis of the membrane arrays data showed significant increases of several key MMPs. Both data sets indicated that IL-6 is important in MSC mobilisation and migration. We also investigated the impact of IL-6 induction on MSCs in 3D spheroid culture, serving as a simplistic model of the bone marrow niche, characterised by fluorescently tagged magnetic nanoparticles and identical membrane antibody arrays. An increase in MMP levels secreted by cells treated with 1 ng/mL IL-6 versus control conditions was noted in addition to migration of cells away from the central spheroid mass.

Keywords: magnetic nanoparticles; matrix metalloprotease; tissue inhibitor of metalloprotease; mesenchymal stem cell; type I collagen; spheroid

1. Introduction

Stem-cell-based therapies have the potential of becoming the future of medicine [1], personalised to the patient [2]. Embryonic stem cells (ESCs) have the highest differentiation potential, offering limitless possibilities for tissue replacement. However, sourcing embryonic stem cells poses ethical concerns, and current UK regulations restrict their availability to the first 14 days, so a more plentiful source of stem cells would be necessary for wide-scale uptake of stem cell therapy. Therefore, the more readily available adult stem cell populations, such as mesenchymal stem cells (MSCs), are of great interest when new therapies and technologies are developed [3].

MSCs derived from the bone marrow niche are multipotent, capable of differentiating into osteoblasts (bone), chondroblasts (cartilage), and adipoblasts (fat) [4]. These precursor cells are essential

to the formation, maintenance, and repair of the skeleton. MSCs are identified by several cell surface markers including the presence of CD105, CD90, and CD73 and the absence of CD45, CD34, CD14, CD19, and HLA-DR [5]. MSCs grown in monolayer will typically begin to lose differentiation potential from around the 6th passage, demonstrating the vital role cell signalling from other supporting cell types within the bone marrow microenvironment plays in maintaining stemness [6,7]. Within the bone marrow microenvironment, the MSC niche can be subdivided into the endosteal and the perivascular niches, where MSC populations are maintained by, and communicate via cytokines, with other cells, such as hematopoietic stem cells (HSCs) and later precursor cells such as osteoblasts and adipoblasts [8–10].

Upon appropriate signalling cues, MSCs mobilise and migrate out from the niche [11]. MSC mobilisation is often due to either (1) homing to sites of injury [12,13] or (2) homing to disseminated tumour cells [14]—both are of key interest to researchers in terms of regenerative medicine (i.e., replacement of lost skeletal tissue) and potential therapeutics for cancer. To date the precise mechanism of mobilisation remains poorly understood.

To gain a deeper understanding of MSC behaviour within the bone marrow microenvironment, it is important to develop more accurate in vitro model systems. One key approach to bring this to fruition is the development of three-dimensional (3D) cell culture model systems. Unlike standard two-dimensional (2D) monolayer cultures, 3D models display nutrient and oxygen gradients, providing a more physiological representation. In addition to this, a more in vivo-like cell behaviour is encouraged, leading to longer culture life spans offering a useful platform for more accurate assessment of drug efficacy during cell cytotoxicity tests [15–17].

The 3D culture adopted in this study utilises MSC internalisation of magnetic nanoparticles (mNPs), prior to levitation in response to an external magnetic field (280 mT), which coerces magnetically labelled MSCs together to form cell aggregates or spheroids. It has been confirmed in multiple studies [18–20] that mNPs do not adversely affect cells and their presence allows cell imaging to be done quickly, without fixation and subsequent staining, as the mNPs are conjugated to, in this case, fluorescein molecules. The spheroids are then cultured within type 1 collagen gels (Figure 1), where MSC spheroids display stem cell-like properties, with cells entering a quiescent state, maintaining a population of multipotent cells capable of responding to modelled wound sites by migration and differentiation [18].

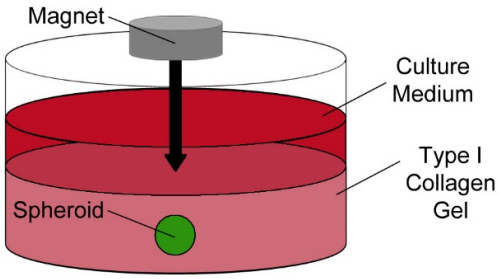

Figure 1. Schematic of three-dimensional spheroid culture. Following its formation, the spheroid is levitated in a type I collagen gel where it can be maintained for several weeks.

Injury or inflammation cause cellular release of cytokines, transforming growth factor-ß (TGF-ß), tumour necrosis factor-α (TNF-α), several interleukins (IL) such as IL-1, IL-6, and IL-10, and the interferons, which all play an important role in controlling the immune response [21]. These cytokines also stimulate the recruitment of MSCs where they initiate tissue repair at the site of the wound [22]. Previously published work from our lab assessed migratory signals produced by artificial wound models [12]. From a panel of several key cytokines (IL-1b, Il-2, TNFα, IL-12p70, and IL-6), only IL-6 was identified as being able to induce MSC migration from the spheroid models [12]. Well known for its roles within inflammation, immune response, and skeletal maintenance, IL-6 is also a key

regulator in cell differentiation, as it is heavily associated with haematopoiesis and differentiation of both osteoblasts and osteoclasts [23–26].

Understanding MSC migration will help inform on potential delivery routes in cancer therapeutics and within the field of regenerative medicine. Cell migration involves the breakdown of extracellular matrix (ECM), which requires the action of proteolytic enzymes such as matrix metalloproteinases (MMPs). There are several classes of MMPs depending on their substrate specificity: (1) collagenases (MP-1, -8, -13, and -18), which cleave fibrillar collagens type I, II, and III, (2) gelatinases (MMP-2 and -9), which cleave gelatin, but can also degrade other extracelluar matrix proteins including collagen and laminin, (3) stromelysins (MMP-3, -10, and -11), which degrade several non-collagenous proteins, and (4) membrane-type MMPs (MMP-14, -15, -16, -17, -24, and -25) [27,28]. MMP activity is regulated by tissue-specific inhibitors of MMPs (TIMPs). The balance between MMPs and TIMPs is critical in ECM remodelling, cell migration, cell differentiation, and the regeneration of any tissue [29]. Therefore, the involvement of these enzymes in MSC migration could provide valuable information with regard to tissue regeneration. In this study, we aim to identify which MMPs are employed in IL-6-induced migration in both 2D and 3D MSC culture by analysing media extracted from monolayer and spheroid cultures. The presence of a panel of seven human matrix metalloproteinases (MMP-1, MMP-2, MMP-3, MMP-8, MMP-9, MMP-10, and MMP-13) was quantified following IL-6 addition into the microenvironment. A panel of three tissue inhibitors of metalloproteinases (TIMPs; TIMP-1, TIMP-2, and TIMP-4) was also assessed, to analyse the relationship between protein and inhibitor following IL-6 sensing by cells. TIMPs directly inhibit MMP protein via binding of the active site [30]. To complement this analysis, monolayer cells were also observed on an Ibidi cell migration plate assay (using time lapse microscopy) over a 24 h period in the presence of IL-6, whilst spheroids were imaged over a series of days both in the presence and absence of IL-6, allowing visualisation of both 2D and 3D migratory response leading to a greater understanding of the migration and giving further insight into the role IL-6 plays within these model systems.

2. Materials and Methods

2.1. Expansion Cell Culture

Human Mesenchymal Stem Cells (Promocell) were cultured using modified DMEM made up of 400 mL of Dulbecco's modified Eagle's medium, 100 mL of media 199, 50 mL of foetal bovine solution, 10 mL of penicillin-streptomycin, and 5 mL of sodium pyruvate. When maintained in culture flasks of MSC cultures were passaged using standard established procedures when confluent and the media refreshed every 3–4 days.

2.2. μ-Slide Chemotaxis 2D

The kit provided by Ibidi allows the measurement of directional movement of a group of cells in response to a chemoattractant. Using the set protocol provided with the '3D Chemotaxis Assay Using μ-Slide Chemotaxis—2.2 2D Chemotaxis Experiments without Gel' slides, MSCs were seeded at 1×10^5. Once both reservoirs were filled with 60 μL of chemoattractant-free DMEM, 30 μL of 1 ng/mL IL-6 was aspirated into the left reservoir to begin the chemoattraction for the assay. The plate was then imaged on a 4× objective lens at 120 s intervals over 24 h at 37 °C. Results were then analysed using the ImageJ plugin 'manual tracking' and Ibidi's own 'Chemotaxis and Migration' tool.

2.3. Preparation of Array Membrane Samples

MSCs were seeded at 5×10^4 in 1 mL of media in a 24-well plate and incubated for 24 h (37 °C and 5% CO_2). Cellular migration was then induced by adding 1 mL of 1 ng/mL IL-6, and cells were incubated for two set time periods—3 h and 24 h. After each set incubation period media was extracted and stored at −20 °C prior to use on Abcam MMP Antibody Array Membranes.

2.4. Generation of Three-Dimensional Spheroid Model System

Spheroids were generated using the methodology as described in Lewis et al. (2016) [12]. Cells were initially seeded at a density of 1×10^4 into a 24-well plate and cultured for 24 h (37 °C; 5% CO_2). After this initial incubation, each well of cells was incubated with 0.1 mg/mL suspension of green fluorescently labelled magnetic iron oxide nanoparticles (chemicell—fluidMAG-PEA with a magnetite core; iron oxide, Fe_3O_4) in 1 mL of DMEM for 30 min (37 °C; 5% CO_2) above a 24-well 280 mT magnetic array plate (Chemicell). After the 30 min incubation, the media was removed and excess iron washed from each well using HEPES saline. Cells were then detached from the surface using trypsin and resuspended in 4 mL of fresh media in a 6-well plate; a magnet 10 mm in diameter (280 mT) was placed on the top of each well, and MSCs were further cultured for 24 h to allow spheroid formation. Once formed, the spheroids were carefully transferred into a type I collagen gel and cultured in 1 mL of fresh media.

2.5. Collagen Gel Preparation

Collagen gels for maintaining and culturing spheroids was made up by initially premixing 0.5 mL of foetal bovine solution, 0.5 mL of modified DMEM culture media, and 0.5 mL of alpha-MEM making up an initial premix of media. Exactly 2.5 mL of rat tail collagen was mixed with 1 mL of 0.1 M NaOH, before mixing with the media premix. Additional NaOH was then titrated dropwise until entire solution turns from yellow/orange to a stable pink, indicating the correct pH change required for gelation. One milliliter of the gel solution was added to individual spheroids within a 24-well plate. A setting period of $\leq$1 h at 37 °C was permitted prior to the addition of fresh culture media.

2.6. Electron Microscopy Preparation

Cell spheroids were generated before fixing in 2.5% glutaraldehyde/0.1 M phosphate buffer fixative for 1 h at room temperature before rinsing in buffer three times for 5 min. Fixed spheroids were treated in osmium tetroxide/0.1 M phosphate buffer for 1 h and washed with distilled water three times for 10 min before being treated in uranyl acetate for 1 h in the dark. Spheroids were then dehydrated in increasing (ethanol) for 10 min until absolute ethanol. Scanning EM samples were then dried in hexamethyldisilazane before they were mounted on SEM stubs. Mounted samples were then coated with 10 nm gold/palladium using a polaron SCS15 SEM coating system. Samples were viewed using JOEL 6400 SEM at 10 kV. Images were false coloured with Adobe Photoshop CS4.

Tunnelling EM sample spheroids were further processed by first washing in propylene oxide three times for 5 min then a 1:1 mix of propylene oxide: araldite/epon 812 resin overnight. These samples were then embedded in fresh araldite resin and set in moulds for 48 h to allow the resin to polymerise. Seventy-nanometer sections were cut using a Leica Ultracut UCT and a Diatome diamond knife at an angle of 6°. Sections were then mounted on 100 mesh formvar-coated copper grids and then contrast-stained with 2% methanolic uranyl acetate for 5 min and with Reynold's lead citrate for a further 5 min before imaging on JOEL 1200 TEM at accelerating velocity of 80 kV.

2.7. Inducing Migration and Preparation of Samples

MSC spheroids were either cultured with DMEM alone as control samples or induced using 1 ng/mL IL-6. Media samples of induced spheroids were extracted and stored at −20 °C on Days 1 and 3 in preparation for use on Abcam MMP Antibody Array membranes. To better understand the cell migratory processes within a 3D cellular spheroid system, spheroids of both IL-6-induced and media-only control samples were also imaged at Days 0, 1, and 3 for qualitative exploration of cellular migration from spheroids using Zeiss Axio Vert A1 flourescence microscope (excitation at 365 nm and emission at 420 nm to detect fluorescein conjugated to mNPs).

2.8. Abcam Human MMP Antibody Array Membranes

Following the protocol in the Human MMP Antibody—Array Membrane 'Instructions for use' booklet media, samples from (i) the 2D MSC IL-6 Induced Samples at 3 and 12 h and (ii) the 3D MSC IL-6 induced samples at Days 1 and 3 were incubated overnight on array membranes at 4 °C. The following day, media samples were aspirated off, and membranes were washed using the supplied buffers and incubated for 2 h at room temperature in 1 mL of biotin-conjugated anti-cytokines. Membranes were then rewashed and incubated in 2 mL of HRP-conjugated streptavidin overnight at 4 °C. Prior to chemiluminescence detection, streptavidin was removed, and membranes were washed a final time. Membranes were then transferred, printed side up, onto provided plastic sheets and detection buffers pipetted onto each sample. After 2 min of incubation, a second plastic sheet was placed on top and membranes were imaged via chemiluminescence detection using a CCD camera with 20 s exposure times.

3. Results and Discussion

MSCs, in a 2D culture, were initially observed to migrate toward an IL-6 gradient in response to IL-6, at a concentration previously noted to induce MSC migration from 3D spheroids (350 pg/mL; [12]). Upon IL-6 exposure, cells were tracked over 24 h using time-lapse light microscopy. A clear directionality was observed toward the IL-6-spiked DMEM, where large filopodia were noted extending in the direction of IL-6, inducing a leading edge and migration (Figure 2) [31]. Cell migration was analysed to assess global migration over 24 h; a rose plot confirmed MSC preferential migration toward IL-6 (positive axis; Figure 3B). A vector plot further supported the motility of each analysed cell from the point of origin (Figure 3A). Thus, MSCs preferentially moved >50 μm toward [IL-6] within the 24 h period.

Cytokines are secreted, principally, by lymphocytes and macrophages. They act by altering the function of target cells in a paracrine or autocrine fashion. However, invading breast cancer cells, within the bone marrow, have been noted to secrete cytokines initiating an epithelial-to-mesenchymal transition leading to a metastatic phenotype. This signalling occurs at very low concentrations (pg/mL–ng/mL) [32]. MSCs are known to respond to TNFα, IFNγ, IL-1, and IL-6 concentration gradients [12,33], permitting movement toward the site of damage [22] through initiation of cell signalling pathways [34].

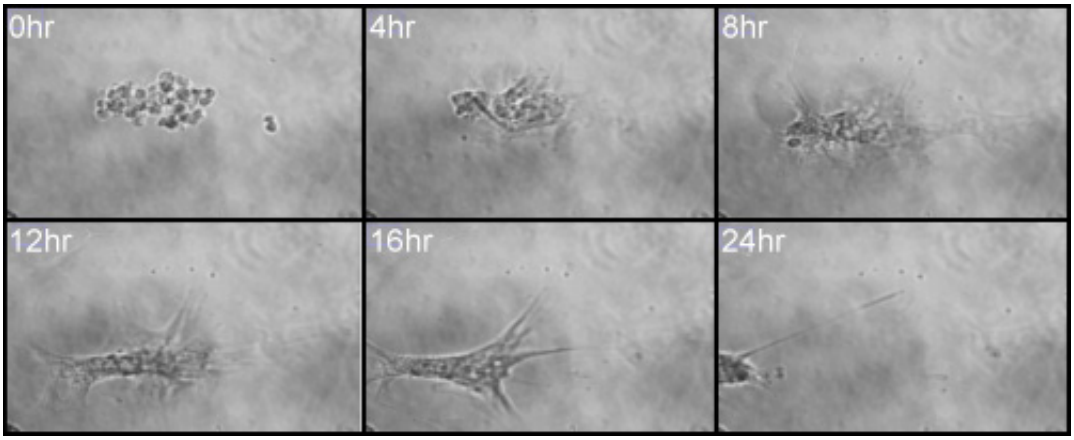

Figure 2. A montage of six images taken from the 24 h time-lapse following a single MSC cultured within an Ibidi μ-Slide Chemotaxis 2D assay plate with IL-6/DMEM (1 ng/mL) in the first reservoir and culture media alone in the reservoir on the right.

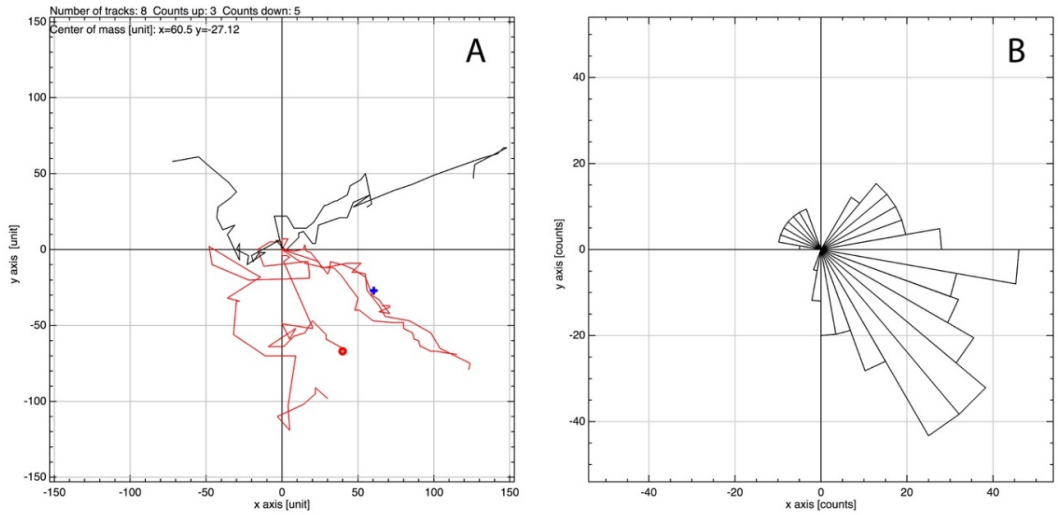

Figure 3. Analysis of images generated during the 24 h MSC time-lapse imaging using the manual tracking plugin for ImageJ and the chemotaxis tool provided by Ibidi. IL-6 containing media was situated toward the positive axis. (**A**) Vector plot based on the tracking of 8 randomly selected cells showing the vector each cell has moved from origin with (**B**) showing the directionality of the cells as a rose plot.

3.1. MMP-1 and MMP-3 Facilitate MSC IL-6-Induced Migration in Monolayer

MSCs were incubated in IL-6 (1 ng/mL); culture media was then collected after 3 h and 24 h and analysed for the presence of matrix metalloproteases (MMPs) and their tissue inhibitors (TIMPs). Changes in MMP/TIMP levels were quantified and expressed graphically (Figure 4). MMP transcription is regulated by cytokines [35]; hence, as the cell is exposed to IL-6, secretion of collagenases MMP-1 and MMP-3 is upregulated. Secretion of the corresponding inhibitor [34], TIMP-1, also rises as a balance is sought to prevent pathological conditions [36]. In this way, IL-6 will facilitate cell migration until it is exhausted. An increase in the MSC rate of migration has previously been described in response to cytokines MCP-1 and IL-8 [37].

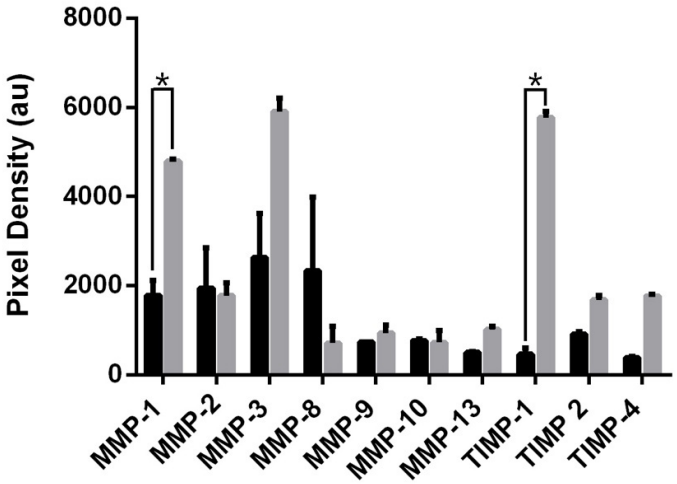

Figure 4. Mean pixel density of target proteins secreted into culture media by IL-6-induced MSCs at 3 h (black) and 24 h (grey) hour intervals. Culture medium was analysed using Abcam human MMP antibody array membranes, viewed on Agilent 2100 Bioanalyser, followed by quantification using ImageJ. Values analysed via *t*-test, * $p < 0.005$.

3.2. Magnetic Nanoparticles Enable MSC Spheroid Culture

The effect of MSC cell seeding density with regard to resultant spheroid size was assessed (Figure 5). Three different seeding densities were used; 6×10^3, 1×10^4, and 2×10^4 cells/mL, with spheroid diameter measured after 24 h in culture medium under 280 mT magnetic field, based on the green fluorescent magnetic nanoparticles within the cells. There was no significant difference ($p > 0.005$) in the mean areas of spheroids (Figure 5D); however, interestingly, spheroid number increased with seeding density, suggesting that the cells have a finite rate of spheroid formation within 24 h. Further characterisation via scanning electron microscopy indicates the close relationship between cells within the spheroid. MSCs become compacted when compared with the monolayer culture, where cell diameter is >50 µm, but here MSCs do not exceed 10 µm and are tightly bound to neighbouring cells (Figure 5E). Tunnelling electron microscopy allows the internal structures of the MSC to be probed. Once internalised, mNPs are retained inside endosomes within the cell cytoplasm (Figure 5F), but do not enter the nucleus and are not toxic to the cell (as shown in previous publications [12,18,38]).

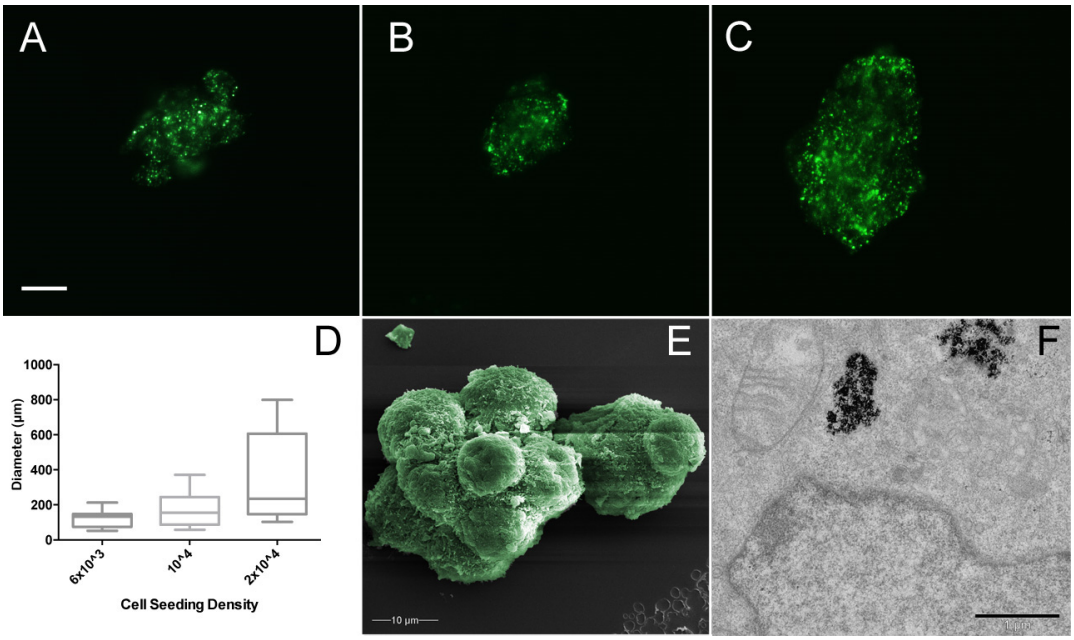

Figure 5. MSC spheroid area derived from cells seeded at (**A**) 6×10^3, (**B**) 1×10^4, and (**C**) 2×10^4 cells/mL. Note the increasing range of spheroid sizes with increased cell density. Scale bar = 10 µm. (**D**) Box and whisker plot of spheroid areas (spheroid $n \geq 15$). (**E**) False colour scanning electron microscopy of MSC spheroid using JEOL JSM-6400 scanning electron microscope at 10 kV. (**F**) Tunnelling electron microscopy of MSC spheroid using JEOL 1200 tunnelling electron microscope at 80 kV; scale bar = 1 µm. Cells labelled with green fluorescent mNPs were levitated in magnetic field for 24 h before measurement. Diameter measured using ImageJ.

3.3. MSCs Migrate in Response to IL-6 in Three-Dimensional Spheroid Culture

Following observations that MSCs migrated in response to an IL-6 gradient in 2D culture, MSC spheroids were observed for cell migration in response to IL-6 over a 3-day period. MSCs were developed into three-dimensional spheroids and levitated in collagen gels, using mNPs, to produce an in vitro culture model the bone marrow microenvironment [12,38]. As noted in Figure 6, following IL-6 exposure, initial MSC migration was observed after 3 h, with very apparent cell migration after 24 h IL-6 exposure.

In vivo, cells would migrate toward the source of IL-6 [39], in the case of this in vitro experiment, there is no singular source of IL-6 (such as co-cultured cells) and concentration is uniform across

the whole culture. MSCs will, therefore, migrate out of the central mass in all directions. Indeed, fluorescent images of these spheroids indicate a migration of cells from the central mass following IL-6 treatment compared with a retention of spheroid shape in the control culture, not treated with the cytokine (Figure 6). Cells within the spheroid therefore appear to sense IL-6, most likely via the cognate cell surface receptor, IL6R [21], and the peripheral cells will transition from adherent cells to a migratory cell phenotype, to move toward the source of IL-6. This was observed in spheroids treated with IL-6, where peripheral cells increase in size as they change morphology to facilitate migration (Figure 6D). It should be noted that MSC spheroids may react to the presence of other MSC spheroids in their vicinity within the collagen gel, so even in control conditions cells may begin to migrate from the mass, but the effect of IL-6 on the migration of MSCs is much more pronounced.

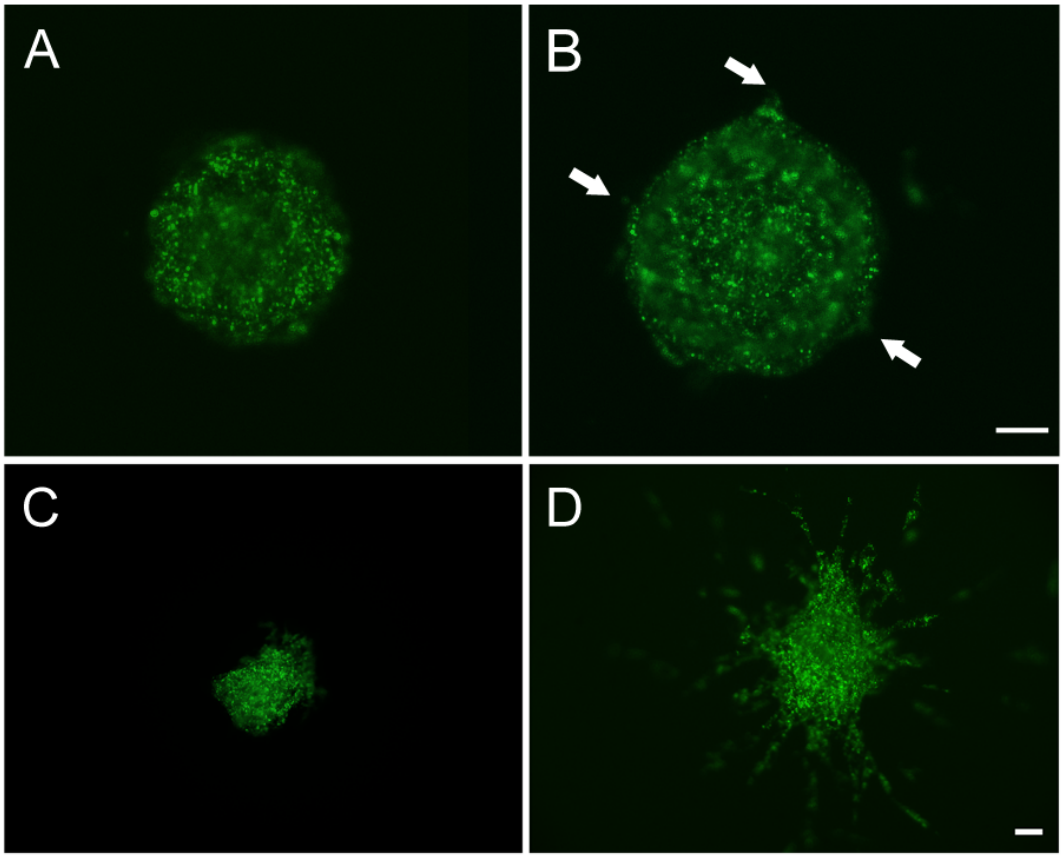

Figure 6. MSC spheroids (10,000 cells/mL) cultured in (**A**) standard media at 3 h; (**B**) 1 ng/mL IL-6 at 3 h; (**C**) standard media at 24 h; (**D**) 1 ng/mL IL-6 at 24 h. Arrows indicate initial cellular migration at 3 h. Green indicates presence of mNPs. Images taken with Zeiss Axio Vert A1 fluorescent microscope (excitation = 365 nm and emission = 420 nm). Scale bar = 10 µm.

3.4. MMP-2 and MMP-8 Facilitate MSC IL-6-Induced Migration in 3D Spheroid Culture

In order for MSCs to migrate, they must change from an adhesive phenotype to a migratory phenotype. The migratory behaviour of MSCS involves MMP activity, with different MMP profiles depending on the migratory reason [29]. Within our system, focusing on MSC migration in response to IL-6, MSC spheroids cultured in standard DMEM indicated an overall decrease in both MMP and TIMP secretion from 1 to 3 days (Figure 7). This correlates with previous evidence that MSCs become quiescent in collagen gels with time and thus do not migrate [18]. However, the MMP secretion profile for MSC spheroids challenged with 1 ng/mL IL-6 is notably different; there is a significant increase in MMP-8 a collagenase specific to types I-III [30]. Interestingly, other collagenases specific to collagen type I, MMP-1 and MMP-13, show no significant change following IL-6 treatment. The only significant

change in TIMP secretion was through an increase in TIMP-4. TIMP-4 is known to interact with MMP-2 [40], a gelatinase, which indicates a significant decrease following IL-6 treatment (Figure 7). The MMP profiles seen in 2D and 3D differ notably in the types of MMP upregulated and the levels with which they change. In monolayer culture, MSCs are only surrounded by ECM laid down themselves and any proteins that may be present in the foetal calf serum within the culture medium. However, in 3D culture, cells are surrounded by type I collagen, making migration much more difficult and thus taxing on the cell, hence why the secretion of some MMPs are downregulated.

MSCs respond to IL-6 in their environment, often secreted by invading cancer cells. IL-6 activates JAK/STAT and MAPK pathways to permit survival and proliferation of MSCs [41]. This leads to the formation of actin stress fibres to facilitate migration [42]. In this way, local MSCs act as a source of fibroblasts to permit tumourigenesis of the neoplastic cells [43]. Therefore, the response of MSCs to paracrine IL-6 is of importance in understanding the growth patterns of disseminated cancer cells.

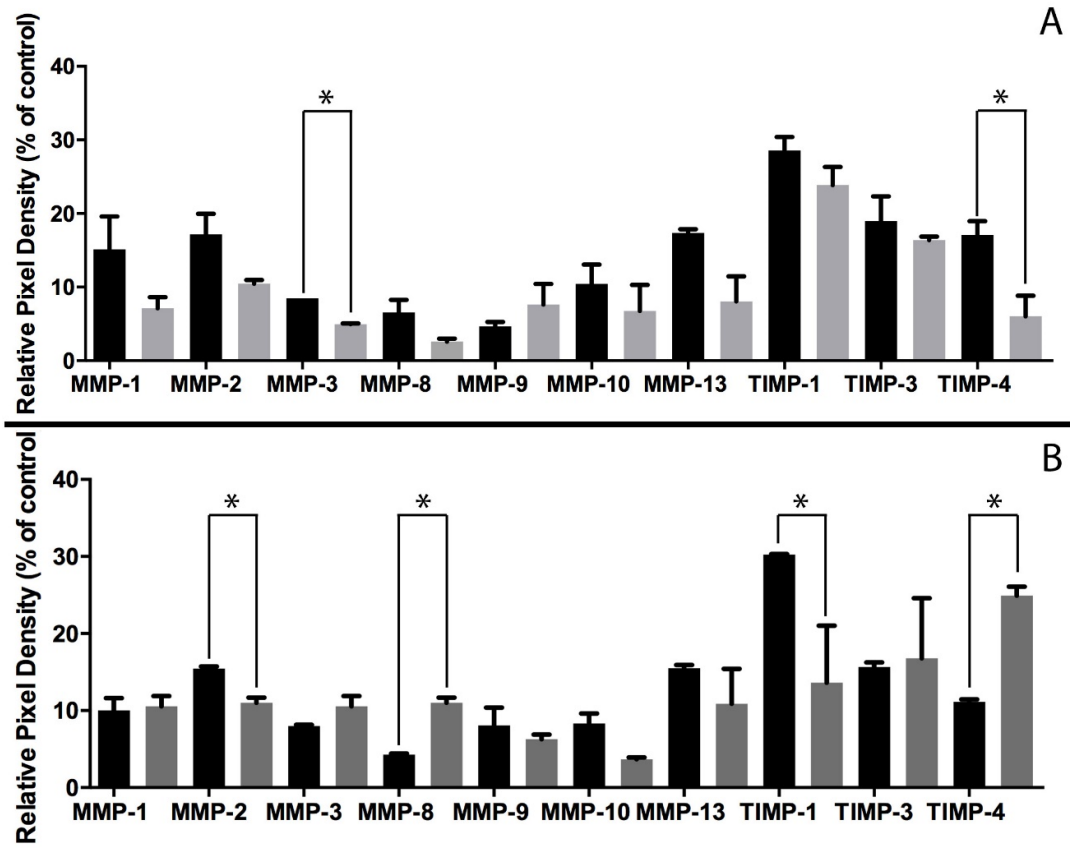

Figure 7. MSC spheroid MMP and TIMP secretion into culture medium at 3 h (black) and 72 h (grey). (**A**) Standard media and (**B**) DMEM with 1 ng/mL IL-6. Protein array membranes viewed using Agilent 2100 Bioanalyser, followed by quantification using ImageJ. Values analysed via *t*-test, * $p < 0.005$.

4. Conclusions

We aimed to use a 3D spheroid culture system to determine whether MSCs migrate toward an IL-6 signal and, if so, what changes in MMP/TIMP secretion profiles facilitate such migration. Cells in vivo will rarely experience conditions such as those of a monolayer culture, as cells in vivo grow in a complex 3D environment. Magnetic nanoparticles facilitated spheroid generation and allowed for the tracking and imaging of MSCs during culture. Our results show not only that MSCs migrate toward IL-6 in both 2D and 3D cultures, but also that, based on a comparison of both culture systems, the secreted MMP profiles change. In a 2D culture, MMP-1 and MMP-3 are secreted during migration, whereas MMP-8 is increased in a 3D spheroid/collagen gel culture. The adoption of a magnetic MSC

spheroid culture therefore provides a simple and effective approach for studying MSC migratory behaviour within a 3D environment; additional studies on other key cytokines would further our knowledge base with regard to MSC migration during wound and tissue healing/regeneration.

Acknowledgments: The authors would like to reference funding from the BBSRC for this work, grant reference number BB/L008661/1.

Author Contributions: C.C.B. conceived and designed the experiments, and assisted in writing the paper; J.C. and S.O. performed the experiments; J.C. and S.O. analysed the data; J.C. wrote the paper; C.-A.S. assisted in the experiments and M.J.D. provided MSCs and expertise in experimental design.

Conflicts of Interest: The authors declare no conflict of interest.

References

1. Nadig, R.R. Stem cell therapy—Hype or hope? A review. *J. Conserv. Dent. JCD* **2009**, *12*, 131–138. [CrossRef] [PubMed]
2. Caplan, A.I.; Bruder, S.P. Mesenchymal stem cells: Building blocks for molecular medicine in the 21st century. *Trends Mol. Med.* **2001**, *7*, 259–264. [CrossRef]
3. Sohni, A.; Verfaillie, C.M. Mesenchymal stem cells migration homing and tracking. *Stem Cells Int.* **2013**, *2013*, 130763. [CrossRef] [PubMed]
4. Baksh, D.; Song, L.; Tuan, R.S. Adult mesenchymal stem cells: Characterization, differentiation, and application in cell and gene therapy. *J. Cell. Mol. Med.* **2004**, *8*, 301–316. [CrossRef] [PubMed]
5. Bühring, H.J.; Battula, V.L.; Treml, S.; Schewe, B.; Kanz, L.; Vogel, W. Novel markers for the prospective isolation of human MSC. *Ann. N. Y. Acad. Sci.* **2007**, *1106*, 262–271. [CrossRef] [PubMed]
6. Dominici, M.L.B.K.; Le Blanc, K.; Mueller, I.; Slaper-Cortenbach, I.; Marini, F.C.; Krause, D.S.; Deans, R.J.; Keating, A.; Prockop, D.J.; Horwitz, E.M. Minimal criteria for defining multipotent mesenchymal stromal cells. The International Society for Cellular Therapy position statement. *Cytotherapy* **2006**, *8*, 315–317. [CrossRef] [PubMed]
7. Bonab, M.M.; Alimoghaddam, K.; Talebian, F.; Ghaffari, S.H.; Ghavamzadeh, A.; Nikbin, B. Aging of mesenchymal stem cell in vitro. *BMC Cell Biol.* **2006**, *7*, 14. [CrossRef] [PubMed]
8. Da Silva Meirelles, L.; Caplan, A.I.; Nardi, N.B. In search of the in vivo identity of mesenchymal stem cells. *Stem Cells* **2008**, *26*, 2287–2299. [CrossRef] [PubMed]
9. Frenette, P.S.; Pinho, S.; Lucas, D.; Scheiermann, C. Mesenchymal stem cell: Keystone of the hematopoietic stem cell niche and a stepping-stone for regenerative medicine. *Annu. Rev. Immunol.* **2013**, *31*, 285–316. [CrossRef] [PubMed]
10. Bara, J.J.; Richards, R.G.; Alini, M.; Stoddart, M.J. Concise review: Bone marrow-derived mesenchymal stem cells change phenotype following in vitro culture: Implications for basic research and the clinic. *Stem Cells* **2014**, *32*, 1713–1723. [CrossRef] [PubMed]
11. Ehninger, A.; Trumpp, A. The bone marrow stem cell niche grows up: Mesenchymal stem cells and macrophages move in. *J. Exp. Med.* **2011**, *208*, 421–428. [CrossRef] [PubMed]
12. Lewis, E.E.L.; Wheadon, H.; Lewis, N.; Yang, J.; Mullin, M.; Hursthouse, A.; Stirling, D.; Dalby, M.J.; Berry, C.C. A quiescent, regeneration-responsive tissue engineered mesenchymal stem cell bone marrow niche model via magnetic levitation. *ACS Nano* **2016**, *10*, 8346–8354. [CrossRef] [PubMed]
13. Hannoush, E.J.; Sifri, Z.C.; Elhassan, I.O.; Mohr, A.M.; Alzate, W.D.; Offin, M.; Livingston, D.H. Impact of enhanced mobilization of bone marrow derived cells to site of injury. *J. Trauma Acute Care Surg.* **2011**, *71*, 283–291. [CrossRef] [PubMed]
14. Hu, C.; Yong, X.; Li, C.; Lü, M.; Liu, D.; Chen, L.; Hu, J.; Teng, M.; Zhang, D.; Fan, Y.; et al. CXCL12/CXCR4 axis promotes mesenchymal stem cell mobilization to burn wounds and contributes to wound repair. *J. Surg. Res.* **2013**, *183*, 427–434. [CrossRef] [PubMed]
15. Bhadriraju, K.; Chen, C.S. Engineering cellular microenvironments to improve cell-based drug testing. *Drug Discov. Today* **2002**, *7*, 612–620. [CrossRef]
16. Edmondson, R.; Broglie, J.J.; Adcock, A.F.; Yang, L. Three-dimensional cell culture systems and their applications in drug discovery and cell-based biosensors. *Assay Drug Dev. Technol.* **2014**, *12*, 207–218. [CrossRef] [PubMed]

17. Antoni, D.; Burckel, H.; Josset, E.; Noel, G. Three-dimensional cell culture: A breakthrough in vivo. *Int. J. Mol. Sci.* **2015**, *16*, 5517–5527. [CrossRef] [PubMed]
18. Lewis, E.E.; Child, H.W.; Hursthouse, A.; Stirling, D.; McCully, M.; Paterson, D.; Mullin, M.; Berry, C.C. The influence of particle size and static magnetic fields on the uptake of magnetic nanoparticles into three-dimensional cell-seeded collagen gel cultures. *J. Biomed. Mater. Res. Part B Appl. Biomater.* **2015**, *103*, 1294–1301. [CrossRef] [PubMed]
19. Berry, C.C.; Curtis, A.S. Functionalisation of magnetic nanoparticles for applications in biomedicine. *J. Phys. D Appl. Phys.* **2003**, *36*, R198. [CrossRef]
20. Khmara, I.; Koneracka, M.; Kubovcikova, M.; Zavisova, V.; Antal, I.; Csach, K.; Kopcansky, P.; Vidlickova, I.; Csaderova, L.; Pastorekova, S.; et al. Preparation of poly-L-lysine functionalized magnetic nanoparticles and their influence on viability of cancer cells. *J. Magn. Magn. Mater.* **2017**, *427*, 114–121. [CrossRef]
21. Yagi, H.; Soto-Gutierrez, A.; Kitagawa, Y.; Yarmush, M.L. Mesenchymal Stem Cell Therapy: Immunomodulation and Homing Mechanisms. In *Stem Cells and Cancer Stem Cells*; Springer: Dordrecht, The Netherlands, 2012; Volume 8, pp. 91–104.
22. Maxson, S.; Lopez, E.A.; Yoo, D.; Danilkovitch-Miagkova, A.; LeRoux, M.A. Concise review: Role of mesenchymal stem cells in wound repair. *Stem Cells Transl. Med.* **2012**, *1*, 142–149. [CrossRef] [PubMed]
23. Roux, S.; Orcel, P. Bone loss: Factors that regulate osteoclast differentiation-an update. *Arthritis Res. Ther.* **2000**, *2*, 451–456. [CrossRef] [PubMed]
24. Yoshitake, F.; Itoh, S.; Narita, H.; Ishihara, K.; Ebisu, S. Interleukin-6 directly inhibits osteoclast differentiation by suppressing receptor activator of NF-κB signaling pathways. *J. Boil. Chem.* **2008**, *283*, 11535–11540. [CrossRef] [PubMed]
25. Marriott, I.; Gray, D.L.; Tranguch, S.L.; Fowler, V.G.; Stryjewski, M.; Levin, L.S.; Hudson, M.C.; Bost, K.L. Osteoblasts express the inflammatory cytokine interleukin-6 in a murine model of Staphylococcus aureus osteomyelitis and infected human bone tissue. *Am. J. Pathol.* **2004**, *164*, 1399–1406. [CrossRef]
26. Grellner, W.; Georg, T.; Wilske, J. Quantitative analysis of proinflammatory cytokines (IL-1β, IL-6, TNF-α) in human skin wounds. *Forensic Sci. Int.* **2000**, *113*, 251–264. [CrossRef]
27. Birkedal-Hansen, H.; Moore, W.G.I.; Bodden, M.K.; Windsor, L.J.; Birkedal-Hansen, B.; DeCarlo, A.; Engler, J.A. Matrix metalloproteinases: A review. *Crit. Rev. Oral Biol. Med.* **1993**, *4*, 197–250. [CrossRef] [PubMed]
28. Page-McCaw, A.; Ewald, A.J.; Werb, Z. Matrix metalloproteinases and the regulation of tissue remodelling. *Nat. Rev. Mol. Cell Boil.* **2007**, *8*, 221–233. [CrossRef] [PubMed]
29. Almalki, S.G.; Agrawal, D.K. Effects of matrix metalloproteinases on the fate of mesenchymal stem cells. *Stem Cell Res. Ther.* **2016**, *7*, 129. [CrossRef] [PubMed]
30. Nagase, H.; Visse, R.; Murphy, G. Structure and function of matrix metalloproteinases and TIMPs. *Cardiovasc. Res.* **2006**, *69*, 562–573. [CrossRef] [PubMed]
31. Mattila, P.K.; Lappalainen, P. Filopodia: Molecular architecture and cellular functions. *Nat. Rev. Mol. Cell Biol.* **2008**, *9*, 446–454. [CrossRef] [PubMed]
32. Arihiro, K.; Oda, H.; Kaneko, M.; Inai, K. Cytokines facilitate chemotactic motility of breast carcinoma cells. *Breast Cancer* **2000**, *7*, 221–230. [CrossRef] [PubMed]
33. Ren, G.; Zhang, L.; Zhao, X.; Xu, G.; Zhang, Y.; Roberts, A.I.; Zhao, R.C.; Shi, Y. Mesenchymal stem cell-mediated immunosuppression occurs via concerted action of chemokines and nitric oxide. *Cell Stem Cell* **2008**, *2*, 141–150. [CrossRef] [PubMed]
34. Sozzani, S.; Luini, W.; Molino, M.; Jílek, P.; Bottazzi, B.; Cerletti, C.; Matsushima, K.; Mantovani, A. The signal transduction pathway involved in the migration induced by a monocyte chemotactic cytokine. *J. Immunol.* **1991**, *147*, 2215–2221. [PubMed]
35. Brew, K.; Dinakarpandian, D.; Nagase, H. Tissue inhibitors of metalloproteinases: Evolution, structure and function. *Biochim. Biophys. Acta* **2000**, *1477*, 267–283. [CrossRef]
36. Yang, E.V.; Bane, C.M.; MacCallum, R.C.; Kiecolt-Glaser, J.K.; Malarkey, W.B.; Glaser, R. Stress-related modulation of matrix metalloproteinase expression. *J. Neuroimmunol.* **2002**, *133*, 144–150. [CrossRef]
37. Wang, L.; Li, Y.; Chen, X.; Chen, J.; Gautam, S.C.; Xu, Y.; Chopp, M. MCP-1, MIP-1, IL-8 and ischemic cerebral tissue enhance human bone marrow stromal cell migration in interface culture. *Hematology* **2002**, *7*, 113–117. [CrossRef] [PubMed]

38. Lewis, N.S.; Lewis, E.E.; Mullin, M.; Wheadon, H.; Dalby, M.J.; Berry, C.C. Magnetically levitated mesenchymal stem cell spheroids cultured with a collagen gel maintain phenotype and quiescence. *J. Tissue Eng*. **2017**, *8*. [CrossRef] [PubMed]
39. Heinrich, P.C.; Behrmann, I.; Haan, S.; Hermanns, H.M.; Müller-Newen, G.; Schaper, F. Principles of interleukin (IL)-6-type cytokine signalling and its regulation. *Biochem. J.* **2003**, *374*, 1–20. [CrossRef] [PubMed]
40. Radomski, A.; Jurasz, P.; Sanders, E.J.; Overall, C.M.; Bigg, H.F.; Edwards, D.R.; Radomski, M.W. Identification, regulation and role of tissue inhibitor of metalloproteinases-4 (TIMP-4) in human platelets. *Br. J. Pharmacol*. **2002**, *137*, 1330–1338. [CrossRef] [PubMed]
41. Rattigan, Y.; Hsu, J.M.; Mishra, P.J.; Glod, J.; Banerjee, D. Interleukin 6 mediated recruitment of mesenchymal stem cells to the hypoxic tumor milieu. *Exp. Cell Res.* **2010**, *316*, 3417–3424. [CrossRef] [PubMed]
42. Menon, L.G.; Picinich, S.; Koneru, R.; Gao, H.; Lin, S.Y.; Koneru, M.; Mayer-Kuckuk, P.; Glod, J.; Banerjee, D. Differential gene expression associated with migration of mesenchymal stem cells to conditioned medium from tumor cells or bone marrow cells. *Stem Cells* **2007**, *25*, 520–528. [CrossRef] [PubMed]
43. Mishra, P.J.; Mishra, P.J.; Humeniuk, R.; Medina, D.J.; Alexe, G.; Mesirov, J.P.; Ganesan, S.; Glod, J.W.; Banerjee, D. Carcinoma-associated fibroblast–like differentiation of human mesenchymal stem cells. *Cancer Res.* **2008**, *68*, 4331–4339. [CrossRef] [PubMed]